2011 American Control Conference
on O'Farrell Street, San Francisco, CA, USA
June 29 - July 01, 2011

Optimal Charging Strategies in Lithium-Ion Battery

Reinhardt Klein[†,‡], Nalin A. Chaturvedi[†], Jake Christensen[†],
Jasim Ahmed[†], Rolf Findeisen[‡] and Aleksandar Kojic[†]

Abstract— **There is a strong need for advanced control methods in battery management systems, especially in the plug-in hybrid and electric vehicles sector, due to cost and safety issues of new high-power battery packs and high-energy cell design. Limitations in computational speed and available memory require the use of very simple battery models and basic control algorithms, which in turn result in suboptimal utilization of the battery. This work investigates the possible use of optimal control strategies for charging. We focus on the minimum-time charging problem, where different constraints on internal battery states are considered. Based on features of the open-loop optimal charging solution, we propose a simple one-step predictive controller, which is shown to recover the time-optimal solution, while being feasible for real-time computations. We present simulation results suggesting a decrease in charging time by 50% compared to the conventional constant-current / constant-voltage method for lithium-ion batteries.**

I. Introduction

There is an increasing trend towards the electrification of the automobile, and most car manufacturers have announced plans to produce plug-in hybrid and electric vehicles. Besides other technological challenges, one important aspect of an electric vehicle is the time needed to recharge the battery pack. Advanced battery management systems need to provide adequate charging strategies for 'refueling' the battery pack in a fast, safe, and reliable manner.

Although it is widely recognized that an appropriate charging strategy of the battery is critical for preventing damage and performance degradation, in general only current and voltage limits are considered during the charging process. As mentioned in [1], voltage limits might be too conservative for new batteries and possibly dangerous for aged batteries due to the changed behavior.

Most charging strategies are ad hoc methods, where certain design parameters determine the major part of some rule based control design. Fast charging of batteries is a popular research topic is the electrochemical community, however, this problem has received very little attention from the controls community. Popular charging strategies are constant-current / constant-voltage (CC/CV), pulse current charging, pulse voltage charging [2], [3], [4], with CC/CV being the most wide-spread method to recharge Li-ion batteries. In [5], [6] some promising charging strategies are presented; however, the maximum performance determined by the electrochemistry of the battery is not approached by those methods.

In an ideal battery, and without limitation of the charging unit, one could pass all the charge needed to bring a battery from one state of charge (SOC) to another SOC instantaneously. Many internal processes of the battery have an influence on the charge transfer capabilities, e.g. finite diffusion rate of lithium ions in the electrolyte, reduction/oxidation of materials other than the active material, and formation of resistive films on the active particle surface. These limitations allow only a finite current to be passed through a battery. The faster the charge transfer is forced to happen, the stronger these processes affect the health of the battery. Cell manufacturers thus always provide additional information about utilization constraints on their cells. These constraints involve limits on the maximum charge/discharge current, limits of lower and upper cut-off voltages, and the operating temperature domain. All these limits are geared towards the CC/CV charging method, and hence are rather conservative, since they are specified for the complete lifetime of the battery. In this paper, we alleviate this problem by presenting an optimal charging strategy based on nonlinear model predictive control (NMPC) techniques to charge the battery in the fastest possible manner, while guaranteeing safety throughout the battery's life.

The rest of the paper is structured as follows. In section II we describe in detail the time-optimal charging problem for Li-ion batteries. The developed optimal control problem is studied in simulations and the main features of the solution are characterized. Based on the observations from section II, in section III we present a NMPC scheme for fast battery charging. The proposed NMPC, while being computationally tractable, is able to recover the time-optimal solution. In section IV we describe the standard charging method CC/CV and compare the results with the time-optimal solution. Finally, section V concludes the presented work and points out future work necessary to improve the current status of battery management systems.

II. Optimal charging strategy

In the following we describe in detail the formulation of the fast battery charging process as a time optimal control problem. First, however, we briefly present the electrochemical model of the battery used in this work.

A. Cell model

The state variables of the macro-homogeneous 1-D electrochemical model of a lithium ion battery are the lithium concentration $c_e(x,t)$ in the electrolyte, the lithium concentration $c_s(x,r,t)$ in the positive and negative electrodes, the potential $\Phi_e(x,t)$ in the electrolyte, the potential $\Phi_s(x,t)$ in the positive and negative electrodes, the ionic current $i_e(x,t)$ in the electrolyte, and the molar ionic flux $j_n(x,t)$ between

[†]{Reinhardt.Klein, Nalin.Chaturvedi}@us.bosch.com, Robert Bosch LLC, Res. & Tech. Center, Palo Alto, CA 94304.

[‡]Otto-von-Guericke University, Institute of Automation Engineering, Magdeburg 39106, Germany.

the active material in the electrodes and the electrolyte. The governing equations are given by (see also [1], [7], [8])

$$\epsilon_e \frac{\partial c_e(x,t)}{\partial t} = \frac{\partial}{\partial x}\left(\epsilon_e D_e \frac{\partial c_e(x,t)}{\partial x} + \frac{1-t_c^0}{F} i_e(x,t)\right), \quad (1)$$

$$\frac{\partial c_s(x,r,t)}{\partial t} = \frac{1}{r^2}\frac{\partial}{\partial r}\left(D_s r^2 \frac{\partial c_s(x,r,t)}{\partial r}\right), \quad (2)$$

$$\frac{\partial \Phi_e(x,t)}{\partial x} = -\frac{i_e(x,t)}{\kappa} + \frac{2RT}{F}\left(1-t_c^0\right)\left(1+\frac{d\ln f_{c/a}(x,t)}{d\ln c_e(x,t)}\right)\frac{\partial \ln c_e(x,t)}{\partial x}, \quad (3)$$

$$\frac{\partial \Phi_s(x,t)}{\partial x} = \frac{i_e(x,t)-I(t)}{\sigma}, \quad (4)$$

$$\frac{\partial i_e(x,t)}{\partial x} = \frac{3\epsilon_s}{R_p} F j_n(x,t), \quad (5)$$

$$j_n(x,t) = \frac{i_0(x,t)}{F}\left(e^{\frac{\alpha_a F}{RT}\eta(x,t)} - e^{\frac{-\alpha_c F}{RT}\eta(x,t)}\right). \quad (6)$$

In Eq. (6), the exchange current density $i_0(x,t)$ and the overpotential $\eta(x,t)$ for the main reaction are modeled as

$$i_0(x,t) = r_{eff} c_e(x,t)^{\alpha_a}(c_s^{\max} - c_{ss}(x,t))^{\alpha_a} c_s(x,t)^{\alpha_c}, \quad (7)$$

$$\eta(x,t) = \Phi_s(x,t) - \Phi_e(x,t) - U(c_{ss}(x,t)) - F R_f j_n(x,t), \quad (8)$$

where $c_{ss}(x,t) \equiv c_s(x,R_p,t)$, $U(c_{ss}(x,t))$ is the open-circuit potential of the active material and $c_s^{\max}$ is the maximum concentration in the active material of each electrode.

The internal temperature is described by [7]

$$\rho^{avg} c_p \frac{dT(t)}{dt} = h_{cell}\left(T_{amb}(t) - T(t)\right) + I(t)V(t) - \int_{0^-}^{0+} \frac{3\epsilon_s}{R_p} F j_n(x,t)\left(U(\bar{c}_s(x,t)) - T(t)\frac{\partial U(\bar{c}_s(x,t))}{\partial T}\right) dx, \quad (9)$$

where $T_{amb}(t)$ is the ambient temperature and $\bar{c}(x,t)$ represents the volume averaged concentration of a particle in the solid phase defined as

$$\bar{c}_s(x,t) = \frac{3}{R_p^3}\int_0^{R_p} r^2 c_s(x,r,t) dr. \quad (10)$$

Utilizing the notation of [1], the initial conditions of the battery model are given by

$$c_e(x,0) = c_e^0(x), \quad c_s(x,r,0) = c_s^0(x,r), \quad T(0) = T^0, \quad (11)$$

and the boundary conditions are given by

$$\frac{\partial c_e(0^-,t)}{\partial x} = \frac{\partial c_e(0^+,t)}{\partial x} = 0 \quad (12)$$

$$c_e(L^-,t) = c_e(0^{sep},t), \quad c_e(L^{sep},t) = c_e(L^+,t), \quad (13)$$

$$\varepsilon_e^- D_e \frac{\partial c_e(L^-,t)}{\partial x} = \varepsilon_e^{sep} D_e \frac{\partial c_e(0^{sep},t)}{\partial x}, \quad (14)$$

$$\varepsilon_e^{sep} D_e \frac{\partial c_e(L^{sep},t)}{\partial x} = -\varepsilon_e^+ D_e \frac{\partial c_e(L^+,t)}{\partial x}, \quad (15)$$

$$\frac{\partial c_s(x,0,t)}{\partial r} = 0, \quad \frac{\partial c_s(x,R_p,t)}{\partial r} = -\frac{j_n(x,t)}{D_s}, \quad (16)$$

$$\Phi_e(L^-,t) = \Phi_e(0^{sep},t), \Phi_e(L^{sep},t) = \Phi_e(L^+,t), \quad (17)$$

$$\Phi_e(0^+,t) = 0, \quad (18)$$

$$i_e(0^-,t) = i_e(0^+,t) = 0, \; i_e(x^{sep},t) = -I(t), \quad (19)$$

$$i_e(L^-,t) = -i_e(L^+,t) = -I(t), \quad (20)$$

where $x^{sep} \in \{0^{sep}, L^{sep}\}$ represents the entire separator domain of the battery. In general, it is difficult to provide consistent initial conditions for the battery model, hence we always initialize the model at some equilibrium state where consistent initial conditions are easily obtained [9].

In the above equations, ϵ_e, ϵ_s, σ, R, R_p, F, α_a, α_c, ρ^{avg}, c_p, h_{cell} and t_c^0 are model parameters and are constant in each region of the cell, while κ, $f_{c/a}$ and D_e are known functions of the electrolyte concentration. Additionally, r_{eff}, R_f, D_s, κ, $f_{c/a}$ and D_e have an Arrhenius-like temperature dependency of the form

$$\Theta(T) = \Theta_{T_0} e^{A_\theta \frac{T(t)-T_0}{T(t)T_0}}, \quad (21)$$

where T_0 is some standard temperature and A_θ is a constant.

The voltage is given by the potential difference in the solid phase at the boundaries of the electrodes

$$V(t) = \Phi_s(0^+,t) - \Phi_s(0^-,t). \quad (22)$$

The model parameters are chosen such that the battery mimics the behavior of a mixed high energy/ high power cell. The main feature of energy cells are thicker electrodes of approximately 200μm, compared to 50μm in power cells. Based on the model parameters, the designed cell has a nominal capacity of 3.5Ah.

B. Problem formulation

Loosely speaking, the control problem considered in this work can be described as calculating the *appropriate* current $I(t)$ to be applied to a cell, which transfers a *given amount of charge* Q from one electrode to the other in the *shortest time* possible, while not *excessively aging* the cell. In the following we will clarify this statement and bring it into a mathematical framework.

The *appropriate* current is considered to be constrained as

$$0 \le I(t) \le I_{\max} \quad (23)$$

for two reasons. First, any charging unit is physically limited to supply a finite amount of current. Secondly, in general a charging unit cannot handle negative currents. Furthermore, the charging current is also constrained by the *given amount of charge* Q as

$$Q = \int_0^{t_f} I(t) dt, \quad (24)$$

where t_f is the final time at which the charging process stops.

Note that, since a battery has a finite capacity, Q has to be chosen such that a solution exists at all. In order to ensure this, we calculate the needed charge such that the cell is charged from the initial equilibrium voltage V_0 to a final equilibrium voltage V_f, where $V_0 \le V_f$, in terms of the bulk state of charge (SOC) of the negative electrode [9] as

$$Q = Q^-(SOC_{V_f}^- - SOC_{V_0}^-), \quad (25)$$

where Q^- is the theoretical capacity of the negative electrode, while $SOC_{V_0}^-$ and $SOC_{V_f}^-$ denote the SOC^- at equilibrium voltages V_0 and V_f, respectively. SOC^- is given by

$$SOC^-(t) = \int_0^{L^-} \frac{\bar{c}_s^-(x,t)}{c_s^{\max,-} L^-} dx = SOC^-(0) + \int_0^t \frac{I(\tau)}{Q^-} d\tau. \quad (26)$$

From (25) and (26) we see that (24) is equivalent to

$$SOC^{-}(t_f) = SOC^{-}_{V_f}. \tag{27}$$

Hence, the input current constraint (24) can be reformulated as a final state constraint (27) on $SOC^{-}(t_f)$.

Since aging of Li-ion batteries is still an active research topic, the term *excessively aging* is more difficult to address. In order to reduce aging of the cell, we introduce constraints on some internal states of the battery that have to be satisfied during the charging process. First, it is widely acknowledged that cells age faster at elevated temperatures, thus we impose a constraint on the maximum temperature by

$$T(t) \leq T_{\max}. \tag{28}$$

Second, we want to avoid regimes where unwanted side reactions become important. These regimes are in general described in terms of overpotential inequalities on η_{sr}. Cathodic side reactions occur whenever $\eta_{sr} < 0$, while anodic side reactions occur whenever $\eta_{sr} > 0$. For a more detailed explanation of overpotentials see [1]. Especially during charging, we want to minimize the lithium deposition side reaction [1], [10], which is a cathodic side reaction and occurs in the negative electrode. Thus, we impose in the negative electrode the constraint

$$\eta_{sr}(x,t) = \Phi_s(x,t) - \Phi_e(x,t) - U_{sr}(x,t) > 0, \tag{29}$$

where $U_{sr}(x,t) = 0$ in this case. Note that this constraint is conservative, since the contribution from an additional term involving the ionic flux of the side reaction is neglected due to unknown reaction kinetics. Similar constraints may be utilized to minimize other undesired side reactions, provided $U_{sr}(x,t)$ of those reactions are known.

Finally, mechanical stress induced from concentration gradients can cause particle fracture [11], [12]. If the battery model includes the governing equations for calculating the stress distribution in the electrodes, one should consider appropriate constraints on the stress distribution. Note that since the relationship between the concentration gradient in the solid phase and the stress required to fracture a particle is still being actively researched [11], [12], constraints on the concentration gradients are not considered in this work.

We are now in the position to formulate the minimum time charging problem in the optimal control framework as

Problem 1: Find the optimal charging current

$$I_{\text{opt}}(t) = \arg\min_{I(t)} \int_0^{t_f} 1 dt \tag{30}$$

$$\begin{aligned} \text{subject to:} \quad & \text{model equations } (1)-(9), (11)-(20) \\ & \text{input constraints } (23), (24) \\ & \text{state constraints } (28), (29) \end{aligned}$$

The solution of Problem 1 is difficult to obtain in the general case for several reasons. The underlying battery model consists of a set of coupled nonlinear partial differential algebraic equations. Furthermore, state and input constraints makes the problem very difficult to analyze. Note that (24) is an integral equality constraint involving both the current profile and the final time.

When considering Problem 1 without (28) and (29) and with a *suitable* upper bound on the current in (23), it can be shown that the solution is given by

$$I_{opt}(t) = I_{max}, t \in [0, \tfrac{Q}{I_{max}} 3600]. \tag{31}$$

If, in addition to (28) and (29), the constraint (23) is also removed, the solution to Problem 1 is actually more difficult to obtain. Assuming the battery model admits a solution for all current profiles, then the solution to Problem 1 is impulsive, since the charge Q is transferred instantaneously. However, the difficulties arise since the model equations do not admit a solution for all current profiles, i.e. the electrolyte concentration can be driven to 0, or the surface concentration in the solid phase can become either 0 or c_{max} before all the charge Q can be transferred.

C. Simulation results

The model equations are implemented in Matlab® and Problem 1 is solved numerically. Considering the complexity of the problem, we decided that a direct solution approach is more appropriate than indirect methods. In our approach we reformulate the optimal control problem as a nonlinear programming problem by parameterizing the control input by a sequence of constant current inputs $I_i, i = \{1, 2, \cdots, n\}$ with a fixed time interval δt for each current. We use the fmincon function to obtain the optimal I_i values which describe the optimal charging profile. Note that, since the total charging time is to be minimized, we initialize the optimizer with a sequence of n current values such that

$$\int_0^t I_i(\tau) d\tau = \sum_{i=1}^{n} I_i \delta t \geq Q. \tag{32}$$

We evaluate the model equations and the constraints only until t_f, where t_f is calculated such that (24) is satisfied. The main benefit of this approach is that the problem to be solved becomes much easier for the optimizer, since the equality constraint (24) is now implicitly taken care of. However, in this approach the unused tail of the sequence I_i becomes larger during the optimization, and a significant amount of time might be spent computing the jacobians w.r.t these unused optimization parameters.

In the following simulations we used V_0 = 3V as the initial equilibrium voltage and V_f = 4.1V as the final equilibrium voltage to which the battery needs to be charged. The temperature is constrained to be lower than T_{max} = 40°C and the current limit is set to I_{max} = 15A. The time discretization is set to δt = 30s. Also, we define the minimum local side reaction overpotential in the negative electrode as

$$\eta_{sr}^{\min}(t) = \inf_x(\eta_{sr}(x,t)). \tag{33}$$

Figure 1 presents simulation results for charging the battery at different ambient temperatures. The minimum charging time at T_{amb} = 25°C and T_{amb} = 10°C is calculated as 14 minutes and 20 minutes, respectively. The optimal charging

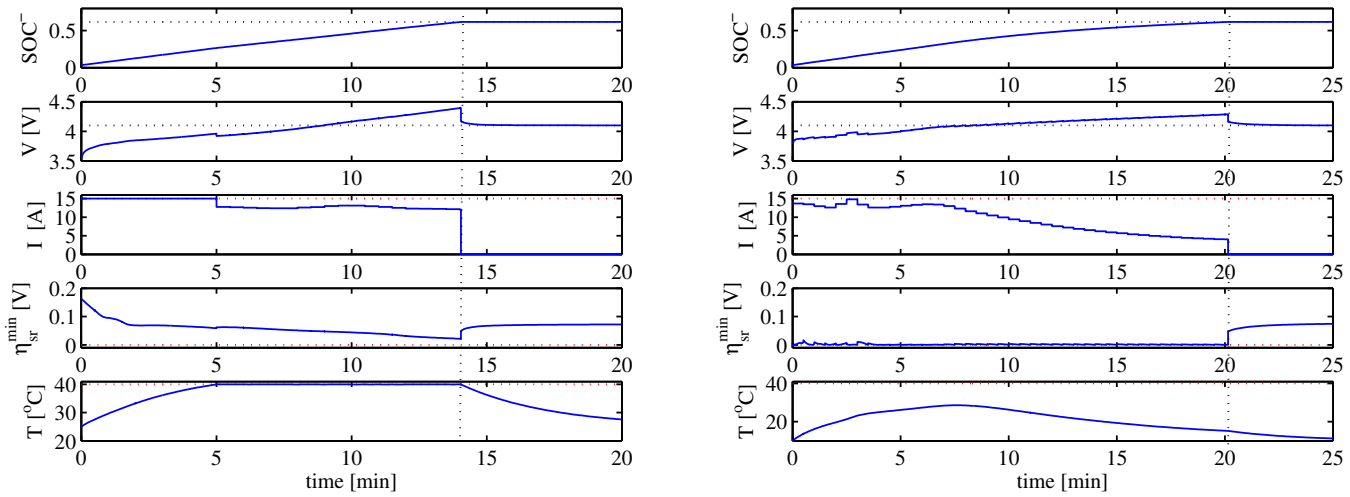

Fig. 1. Simulation results with the optimal current profile obtained by solving Problem 1 with T_{amb} = 25°C (left) and T_{amb} = 10°C (right). Note that the time-optimal charging profile for both ambient temperatures consists of several arcs described by active inequality constraints. After the charging process, we set $I(t)$ = 0 and let the battery relax to the final equilibrium state.

profile obtained at T_{amb} = 25°C consists of two arcs, both determined by inequality constraints of Problem 1. During the first 5 minutes of the charging process the current is limited by (23). The rest of the charging profile is determined such that the constraint (28) is not violated, i.e. the battery is kept at a constant temperature. Note that, in this case, the optimal current profile is discontinuous at the intersection of the constraints (23) and (28). Furthermore, at T_{amb} = 25°C the kinetics of the battery are fast enough such that constraint (29) is not active during the whole charging process.

As depicted in Fig. 1, the optimal charging profile at T_{amb} = 10°C consists of three arcs. The first and the third arc are determined by (29). During charging, the increased temperature leads to faster kinetics and a lower impedance of the battery. The lower impedance allows higher currents to be passed and, for a very brief period, constraint (23) becomes active.

In both charging scenarios the optimal current profile satisfies (24), as can be seen in the SOC subplot in Fig. 1. Note that the transient voltage in both charging scenarios is for a prolonged time higher than V_f. However, after charging is stopped, the voltage relaxes to the desired equilibrium V_f.

The numerical solution of Problem 1, although it reveals some interesting features, is impractical for online implementation, since the computational time for obtaining the optimal charging profile on a 1.8GHz PC is several hours. Furthermore, disturbances will degrade the performance of the open-loop solution, possibly causing constraint violations. In the next section we introduce a feedback algorithm that approximates the open-loop solution while being computationally feasible for real-time control.

III. Closed-loop charging strategy

Based on the numerical solutions of Problem 1 presented in the previous section, we now propose an algorithm to approximate the solution of the optimal control problem. The time-optimal solution is given such that, at all time, the maximum current, which does not violate any constraints, is applied to the battery. Based on this observation, we propose a simple one-step predictive controller. The optimal current profile is approximated in time by a piece-wise constant profile for each time interval δt. At each time instant we calculate from model predictions the maximum current, which does not violate the constraints (23), (29), and (28). Then we apply this current to the battery and move forward in time. Since the time interval δt might be smaller than the total time needed to transfer the charge, we need to abandon the equality constraint (24). Instead of (24), we reformulate this constraint in terms of the desired final SOC as

$$SOC^{-}(t) \leq SOC^{-}_{V_f}, \quad \forall\ t. \tag{34}$$

The algorithm described above fits perfectly in the NMPC scheme [13], where we set the prediction horizon to δt. Since we want to maximize the current applied to the cell, in the proposed NMPC scheme the following open-loop optimal control problem is solved at each time step

$$Problem\ 2: \qquad \min_{I(t)} \int_{t}^{t+\delta t} -I(\tau)d\tau \tag{35}$$

$$\begin{aligned} \text{subject to:} \quad & \text{model equations } (1)-(9), (11)-(20) \\ & \text{input constraints } (23) \\ & \text{state constraints } (28), (29), (34). \end{aligned}$$

Note that feedback is introduced in the NMPC scheme by the new initial conditions (11) at each time step. Since we approximate the current by a single constant, Problem 2 is much easier to solve, and in general we obtain a solution in less than 1 second. It is worth mentioning that in this work we assume all states as measurable. The output feedback NMPC problem using a modified version of the observer presented in [9] for providing the NMPC with the full state information is under investigation by the authors.

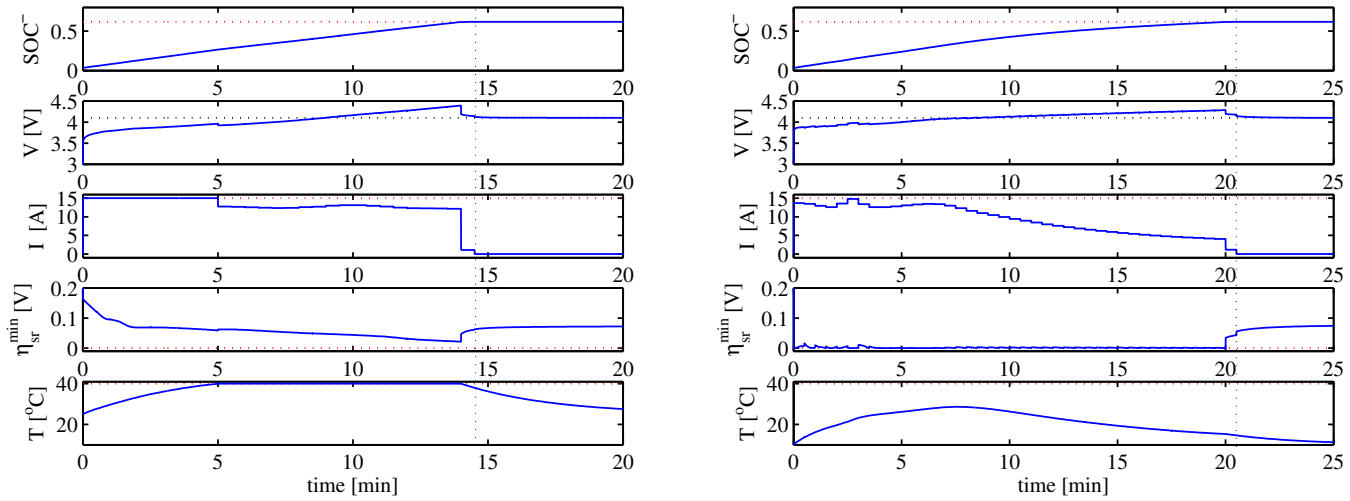

Fig. 2. Simulation results applying the NMPC scheme with T_{amb} = 25°C (left) and T_{amb} = 10°C (right). Note that the current profile only differs for the last step in the NMPC scheme from the time-optimal solution obtained by solving Problem 1 (see Fig. (1)). Beginning from the last non-zero current value, the remaining current profile is due to the SOC constraint (34).

Figure 2 presents simulation results with the NMPC scheme for charging the battery at 25°C and 10°C ambient temperature. For comparison with the open-loop solution, we set the prediction horizon to δt = 30s. As can be seen in Fig. 2, the charging profile obtained by the NMPC is almost identical with the open-loop solution of Problem 1 in Fig. 1. The obtained charging profiles differ only at the end of the charging process, where the charging current amplitude in the NMPC scheme is determined such that the final SOC constraint (34) is not violated. Note that, when charging with the proposed NMPC scheme, a zero current is generated once the final SOC is reached, since any positive charging current would violate the constraint (34).

IV. Standard Charging Method

The most widely used method for charging Li-ion batteries is the constant current - constant voltage (CC/CV) method [2]. As the name of the method already reveals, in this algorithm the battery is charged in CC mode with a constant current until an upper, predefined voltage limit V_{cut}. At this point, the controller is switched to CV mode with the upper voltage limit as setpoint. The charging process is terminated either after a predefined time in CV mode, or when the charging current in CV mode drops to values smaller than a predefined value I_{cut}. Note that while charging in CV mode $I(t) \to 0$ for $t \to \infty$. Hence, the smaller I_{cut} is chosen, the longer the charging time will be.

In order to compare the CC/CV method with the minimum time charging method we set $V_{cut} = V_f$. Also, we choose I_{cut} to be 0.35A which corresponds to a C/10 current; see [1] for details on C-rate. Although the typical current amplitude in CC mode is C/3, some manufacturers allow their batteries to be charged at rates as high as 1C, which for our design corresponds to 3.5A. The current in CC mode is a compromise between faster charging and minimizing aging. Since we have full information on internal states of our battery, we can choose an aggressive charging current in CC mode, which does not violate the proposed constraints. For illustration purposes we also present simulation results with slightly higher charging currents in CC mode. While a higher CC current indeed reduces the total charging time, we show that the constraints are violated in such situations.

Figure 3 presents simulation results with the CC/CV method for different scenarios. The total charging time at T_{amb} = 25°C with CC currents of 13A and 15A is 29 minutes and 27 minutes, respectively. Note that, while charging with 15A is only 2 minutes faster, the temperature constraint is violated for more than 6 minutes during the charging process. At such aggressive charging currents, the battery reaches the upper cut-off voltage V_{cut} relatively fast, and the controller is for most of the time in CV mode. Also, since the charging process is stopped when the current in CV mode becomes smaller than I_{cut}, the charging of the battery is incomplete, i.e. the relaxed voltage of the cell is smaller than V_f since the final SOC is not reached. In Fig. 3 we also present results of the CC/CV method at T_{amb} = 10°C. The charging time at 10°C with CC currents of 6A and 9A is 50 minutes and 43 minutes respectively. Notice that, for the 9A CC current, the side reaction constraint (29) is violated for almost 3 minutes, which damages the battery and is potentially unsafe.

Compared with the time optimal solution of 14 minutes at T_{amb} = 25°C and 20 minutes at T_{amb} = 10°C presented in the previous sections, the CC/CV method needs more than double the time to charge the battery even if very aggressive charging currents in CC mode are utilized. Note that, since the CC currents are fixed, these currents will eventually violate the constraints after the cell starts to deteriorate [1].

It is worth mentioning, that there are many different flavors of the CC/CV method, where, for example, $V_{cut} > V_f$ and I_{cut} is larger. As can be seen in Fig. 3, the CC mode at T_{amb} = 10°C with a 6A CC current is already longer than the complete charging process using the time-optimal charging profile. A more aggressive V_{cut} cannot decrease the total

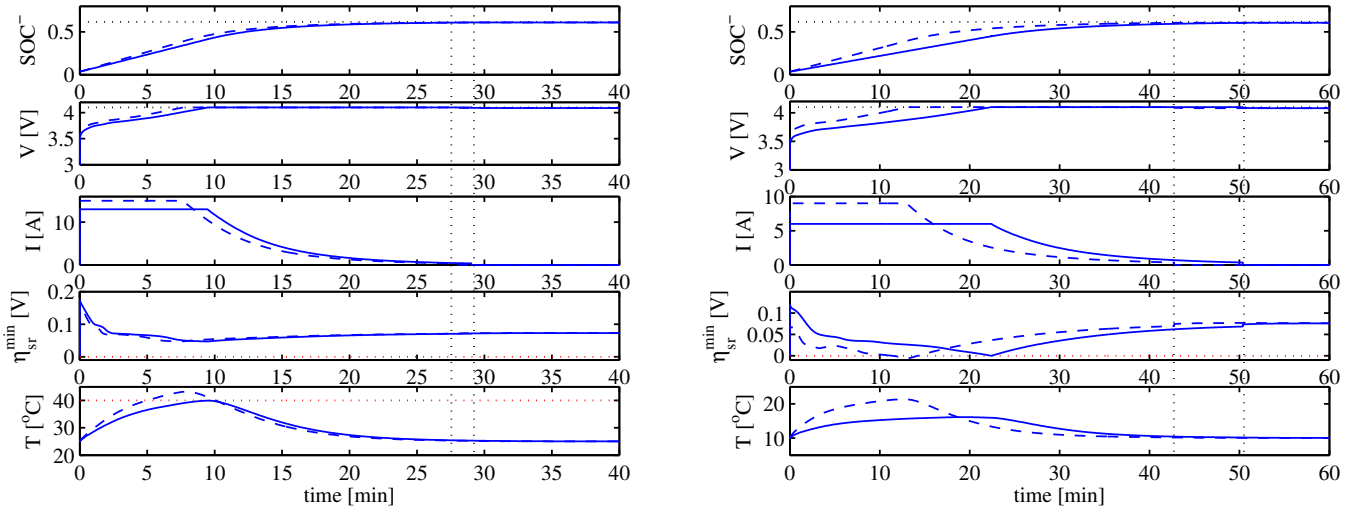

Fig. 3. Simulation results using the CC/CV method with T_{amb} = 25°C (left) and T_{amb} = 10°C (right). At T_{amb} = 25°C a CC current of 13A charges the battery in 29 minutes, while a larger CC current of 15A charges the battery in 27 minutes but violates the temperature constraint (28). At T_{amb} = 10°C a CC current of 6A charges the battery in 50 minutes, while a larger CC current of 9A charges the battery in 40 minutes but violates the side reaction constraint (29). Note that, since $I_{cut} > 0$, the charging is incomplete, as can be seen by a relaxed voltage value less than V_{cut}.

charging time significantly, since a smaller CC current needs to be chosen, such that (29) is not violated.

Regardless of all drawbacks, the CC/CV method is nevertheless the standard charging method because of its simplicity. The main advantage is that no model information is needed to charge the battery. Furthermore, the CC control and the CV control can be realized with very simple circuits, keeping the costs of the charger to a minimum.

V. Conclusions

In this work we presented in detail the optimal control problem for charging a battery in minimum time. Given the complexity of the electrochemical model of the battery, we focused on the numerical investigation of the optimal control problem. We have shown that the optimal charging profile is described by several arcs, where different inequality constraints describing the problem are active. Based on these observations, we propose a one-step model predictive controller which is able to recover the open-loop minimum time solution. The proposed state-feedback NMPC scheme is computationally less prohibitive and feasible for real-time control. The time-optimal charging profiles are compared with the standard CC/CV method for charging Li-ion batteries. While the CC/CV method is very simple to realize in hardware, this method is far from being optimal. Furthermore, considering aging of the battery, the CC currents are in general chosen very conservative, such that safety can be guaranteed during the life-time of the battery.

As part of our research work, we are currently investigating the output-feedback NMPC scheme for the optimal utilization of batteries. Since the performance of the NMPC scheme strongly depends on the quality of the underlying model, a separate parameter estimation is needed to account for parameter changes due to aging of the battery. Along with state and parameter estimation schemes, work is centered around the experimental validation and the robustness of the algorithms utilized in advanced battery management systems.

References

[1] N. Chaturvedi, R. Klein, J. Christensen, J. Ahmed, and A. Kojic, "Algorithms for Advanced Battery Management Systems: Modeling, estimation, and control challenges for lithium-ion batteries," *IEEE Control Systems Magazine*, vol. 30, no. 3, 2010.

[2] P. Notten, J. O. het Veld, and J. van Beek, "Boostcharging li-ion batteries: A challenging new charging concept," *Journal of Power Sources*, vol. 145, no. 1, pp. 89 – 94, 2005.

[3] B. K. Purushothaman and U. Landau, "Rapid charging of lithium-ion batteries using pulsed currents," *Journal of The Electrochemical Society*, vol. 153, no. 3, pp. A533–A542, 2006.

[4] K. Smith, "Electrochemical control of lithium-ion batteries [applications of control]," *Control Systems Magazine, IEEE*, vol. 30, no. 2, pp. 18 –25, apr. 2010.

[5] Y.-F. Luo, Y.-H. Liu, and S.-C. Wang, "Search for an optimal multistage charging pattern for lithium-ion batteries using the taguchi approach," jan. 2009, pp. 1 –5.

[6] Y.-H. Liu, J.-H. Teng, and Y.-C. Lin, "Search for an optimal rapid charging pattern for lithium-ion batteries using ant colony system algorithm," *Industrial Electronics, IEEE Transactions on*, vol. 52, no. 5, pp. 1328 – 1336, oct. 2005.

[7] K. Thomas, J. Newman, and R. Darling, "Mathematical Modeling of Lithium Batteries," *Kluwer Academic/Plenum Publishers*, pp. 345–392, 2002.

[8] M. Doyle, T. F. Fuller, and J. Newman, "Modeling of Galvanostatic Charge and Discharge of the Lithium/Polymer/Insertion Cell," *Journal of The Electrochemical Society*, vol. 140, no. 6, pp. 1526–1533, 1993.

[9] R. Klein, N. Chaturvedi, J. Christensen, J. Ahmed, R. Findeisen, and A. Kojic, "State estimation of a reduced electrochemical model of a lithium-ion battery," *Proc. of the American Control Conference*, 2010.

[10] P. Arora, M. Doyle, and R. E. White, "Mathematical modeling of the lithium deposition overcharge reaction in lithium-ion batteries using carbon-based negative electrodes," *Journal of The Electrochemical Society*, vol. 146, no. 10, pp. 3543–3553, 1999.

[11] J. Christensen and J. Newman, "Stress generation and fracture in lithium insertion materials," *Journal of Solid State Electrochemistry*, vol. 10, pp. 293–319, 2006.

[12] J. Christensen, "Modeling diffusion-induced stress in li-ion cells with porous electrodes," *Journal of The Electrochemical Society*, vol. 157, no. 3, pp. A366–A380, 2010.

[13] R. Findeisen, L. Imsland, F. Allgöwer, and B. Foss., "State and output feedback nonlinear model predictive control: An overview," *European Journal of Control*, vol. 9, no. 2-3, pp. 190–207, 2003.